IEEE Access
Multidisciplinary | Rapid Review | Open Access Journal

Received June 18, 2019, accepted June 23, 2019, date of publication June 26, 2019, date of current version July 15, 2019.

Digital Object Identifier 10.1109/ACCESS.2019.2925046

A Method for Diagnosing Mechanical Faults of on-Load Tap Changer Based on Ensemble Empirical Mode Decomposition, Volterra Model and Decision Acyclic Graph Support Vector Machine

YUQIN XU[1], CONG ZHOU[1], JIANGHAI GENG[1], SHUGUO GAO[2], AND PING WANG[1]
[1]Hebei Provincial Key Laboratory of Power Transmission Equipment Security Defense, North China Electric Power University, Baoding 071003, China
[2]State Grid Hebei Electric Power Research Institute, Shjiazhuang 050021, China

Corresponding author: Cong Zhou (hd15176236798@163.com)

This work was supported by the Key Technology Research Project of Heibei Electric Power Corporation of SGCC.

ABSTRACT A method combined ensemble empirical mode decomposition, Volterra model and decision acyclic graph support vector machine was proposed to improve adaptability, feature resolution, and identification accuracy when diagnosing mechanical faults in an on-load tap changer of a transformer. In detail, the ensemble empirical mode decomposition algorithm was applied to decompose the multi-channel vibration signals in the switchover process of the on-load tap changer. Then, a Volterra model for the mechanical state of the on-load tap changer was established based on time-frequency characteristics obtained through the use of the ensemble empirical mode decomposition algorithm. Moreover, a matrix of coefficient vectors was also used in the Volterra model. This method will not only reduce the aliasing effect of empirical mode decomposition but also obtain high-resolution characteristics of nonstationary vibration signals. Furthermore, taking the singular values of the Volterra coefficient matrix as the fault characteristic, the data states of the model for diagnosing the on-load tap changer were automatically classified and identified by establishing a rapid, multi-classification decision acyclic graph support vector machine model with a low misjudgment rate. Finally, based on a certain on-load tap changer, the test platform for simulating mechanical faults was built. On this basis, by using the proposed method, the vibration signals generated due to typical mechanical faults, such as loosening of moving contacts, lessening of transition contact, and motor jam were acquired and analyzed, thus validating the effectiveness of the method through case studies. Compared with other methods, the new method could overcome many defects in existing methods and it has higher fault identification accuracy.

INDEX TERMS Mechanical variables measurement, signal processing algorithms, fault diagnosis, electromechanical devices, support vector machines, power transformers, switches, time series analysis.

I. INTRODUCTION

On-load tap changer (OLTC) is an important part guaranteeing on-load tap changing transformers (OLTCTs) can realize voltage regulation, so its reliability directly influences the safe and stable operation of OLTCTs and allied power transmission and distribution networks [1]. OLTC is the only movable part of OLTCTs. With increasing voltage regulation operations, the fault rate of it increases compared with that of the other parts. Statistical data show that mechanical faults (including loose contacts, spindle jamming, and spring failure) are the main fault types in OLTCs, accounting for more than 95% of all faults [2]. Mechanical faults can directly damage OLTCs and OLTCTs, further triggering other faults, affecting their electrical performance and leading to serious consequences [3]. Therefore, it is important to explore effective methods to detect mechanical faults in OLTCs. This could ensure the safe and stable operation of the power.

The associate editor coordinating the review of this manuscript and approving it for publication was Gerard-Andre Capolino.

In the fault detection of electrical equipment, methods such as detecting the action time, applying the position sensors or the ultrasonic sensors are relatively common, but they are not suitable for the detection of mechanical faults of the OLTC. According to test results, there is no significant difference in the time required for tap changing under different working conditions [2]. Therefore, it is not feasible to use the switching time to diagnose the mechanical failure of the on-load tap-changer. At the same time, mechanical failures such as loose contacts do not cause significant positional changes in the OLTC contacts. Therefore, it is also not feasible to use position sensors to detect OLTC mechanical faults. Studies show an ultrasonic signal may be generated when a partial discharge occurs inside the transformer [4]. The ultrasonic signal would propagate outward through insulating oil, windings, separators, oil paper, etc. Therefore, if an ultrasonic sensor is used to detect the mechanical faults of the OLTC, it is highly susceptible to interference from ultrasonic waves generated by partial discharge inside the transformer. Vibration analysis is currently the common method for diagnosing mechanical faults of OLTC. The use of the vibration analysis method allows a complete inspection of the internal mechanical state of the OLTC without the need to disassemble the OLTC [2]. It can greatly improve the maintenance staffs' work efficiency and troubleshooting accuracy, which will effectively reduce the power outage time.

How to extract reasonable and effective features from vibration signals is the key of vibration analysis method. In related studies, Kang and Birtwhistle [5], Gan *et al.* [6] used wavelet analysis to extract time-domain characteristics of vibration signals (including peak time and amplitude). In addition, self-organizing mapping and genetic algorithm (GA) were applied to compare the characteristics in normal state with those in fault state to establish OLTC vibration signal database, so as to obtain the evaluation criteria of typical OLTCs working state. However, the actual vibration signal of OLTCs has strong real-time and randomness, and the traditional time-frequency analysis method cannot identify the time-domain information, which has poor adaptability. From the perspective of chaos characteristics of OLTC vibration signals, Zhou and Wang [7] reconstructed vibration signals in high-dimensional space and defined stage distribution coefficients to determine normal and fault states of power grid. However, the definition of evaluation criteria ignored the vector characteristics of reconstructed signals, so there was only a limited fault diagnosis capability. By contrast, P. Chen *et al.* effectively made up for this shortfall. They used the K-means algorithm to cluster the reconstructed signals, and diagnosed the changes of mechanical faults according to the deviation of the center vector of clustering [8]. However, due to the limitations of the clustering algorithm itself, the reconstruction information could not be completely reflected. Therefore, the feature resolution and accuracy of the clustering algorithm are poor when detecting the characteristics of vibration signals. Through empirical mode decomposition (EMD) algorithm, Li *et al.* [1] decomposed vibration signals and diagnosed mechanical faults of OLTC through its frequency domain characteristics. However, due to the significant Mode Mixing effect of EMD algorithm when processing instantaneous nonlinear signals, the decomposition results are not very accurate. To solve this problem, Duan and Wang [2], inspired by integrated ensemble empirical mode decomposition (EEMD) [9], proposed a narrowband noise-assisted multivariable EMD (NA-MEMD) method to obtain the time-frequency characteristics of multi-channel vibration signals during OLTC switching. In addition, they also proposed to use the power matrix similarity index to detect mechanical faults on OLTCs. This method overcomes some shortcomings of traditional methods and has high fault diagnosis efficiency. However, this method relies on matrix similarity to judge fault types, and the judgment index is relatively single, which is easy to cause misjudgment.

To improve adaptability, feature resolution and identification accuracy when diagnosing mechanical faults in an OLTC, a method combined EEMD, Volterra Model and Decision Acyclic Graph Support Vector Machine (DAG-SVM) was proposed. In this paper, the Volterra model for chaotic time series was firstly applied to OLTC fault diagnosis, which could efficiently process non-stationary signals. Based on this, a new feature extraction method combining EEMD and Volterra model was proposed, which has high adaptability and feature resolution. Moreover, The DAG-SVM multi-classification model was applied to identify OLTC mechanical faults, which could realize the pattern recognition and automatic division of various mechanical faults of OLTC. Finally, an OLTC mechanical fault test platform was built, which could simulate some typical mechanical faults, such as loosening of moving contacts, lessening of transition contact and motor jam. Based on test platform, the new OLTC mechanical fault diagnosis method was verified by experiments.

II. THE THEORETICAL BASIS OF THE NEW METHOD FOR DIAGNOSING MECHANICAL FAULTS OF OLTC

As the only movable part of the transformer, a switch progress of the on-load tap-changer contains a series of action events. In this progress, the contact collision, friction and other components are accompanied by the generation of mechanical vibration signals [2]. Typically, these vibration signals can be used for time-frequency vibration analysis. When there are some hidden troubles in the OLTC, the vibration signal of the OLTCT surface will be different from the normal state [2]. Therefore, the vibration waveforms of these motion processes are recorded and analyzed, which can effectively reflect the operating conditions of the OLTC.

The proposed method for diagnosing mechanical faults of OLTC is a combination of EEMD, Volterra Model and DAG-SVM. Among them, EEMD and Volterra Model can realize feature extraction of OLTC vibration signals, while DAG-SVM can realize pattern recognition of multiple faults. The overall flow chart of the method is shown in Figure 1.

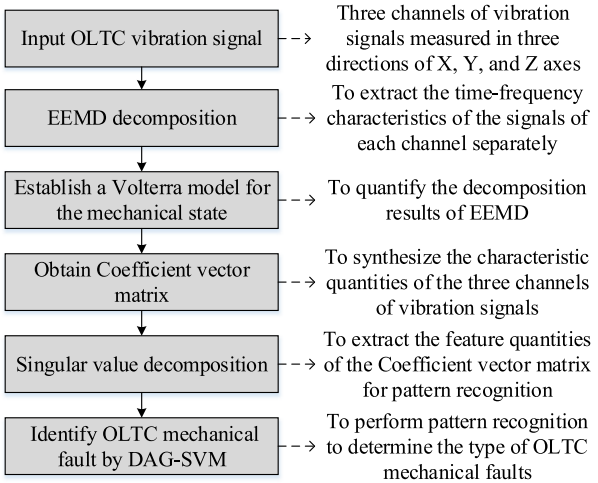

FIGURE 1. Method for diagnosing mechanical faults in OLTC based on EEMD-Volterra and DAG-SVM. This figure illustrates the steps of the method proposed in this paper and the purpose of each step.

1) The three channels of vibration signals during the OLTC switching process are measured by the vibration sensors from three directions of X, Y, and Z axes;
2) EEMD is a time-frequency analysis method that decomposes a single-channel vibration signal into a series of components to extract its time-frequency characteristics;
3) The Volterra model is a prediction method of phase space reconstruction. Its coefficient vector matrix can quantize the time-frequency information contained in the signal. The singular values of the matrix can be used as the characteristic parameters of pattern recognition;
4) DAG-SVM is a multi-class classification model that enables pattern recognition of fault types.

A. ENSEMBLE EMPIRICAL MODE DECOMPOSITION

The vibration analysis method of the OLTC generally includes two parts: feature extraction and pattern recognition. Feature extraction of vibration signal is the key to identify mechanical faults of on-load tap changers. The vibration signal of on-load tap changer is a typical transient non-stationary signal, so the traditional Fourier transform is obviously not suitable for vibration signal processing because of the resolution problem [5]. Meanwhile, Wavelet analysis has the shortcomings of energy leakage and non-adaptability [6]. Thus, Empirical Mode Decompositio9n (EMD) [1] is introduced into vibration signal processing of on-load tap changer mechanical.

EMD decomposition can decompose the collected vibration signals into several IMF components according to the characteristics of the on-load tap changer vibration signals. Therefore, EMD decomposition is very suitable for the processing of nonlinear and non-stationary vibration signals [1]. By using an EMD method, signals were decomposed into a series of intrinsic mode functions (IMFs) whose amplitude and phase vary with time. IMFs need to satisfy two conditions [1]: firstly, the number of zeros is equal to that of poles, or the difference between the two numbers must be no more than 1; secondly, the upper and lower envelope lines are partly symmetric with respect to the timeline. Based on the EMD method, IMF components of multi-component signals at different orders can be screened. Each IMF component reflects the characteristics of an intrinsic mode of original signals (narrowband signals) at different time-scales, and therefore instantaneous frequency exhibits definite physical significance.

Starting from the signal characteristics, the EMD algorithm first extracts the high-frequency IMF with the smallest time feature scale from the signal. Then it separates the low-frequency IMF with large time feature scale layer by layer, and finally obtains the residual component according to the stopping principle. If the original signal is $s(t)$, then its EMD decomposition process is [1]:

1) Primary selection: this step uses cubic spline interpolation. That is, connecting the maximum value of the original signal to obtain the upper envelope, and connecting the minimum value of the original signal to obtain the lower envelope. The average value $m(t)$ of the upper and lower envelopes is then calculated and rejected in the original signal. The result is taken as the initial value $h_1(t)$ of the IMF, namely:

$$h_1(t) = s(t) - m(t) \tag{1}$$

2) Verification: this step verifies whether $h_1(t)$ could meet the requirements of the IMF. If not, import $h_1(t)$ into the first step for further calculation until the result could meet the requirements. At this time, the result is an IMF component, which is denoted as c_1.
3) Loop: this step takes $r_1(t) = x(t) - c_1$ as the new input signal and loops through the first two steps until the input signal is less than a threshold value *res* or becomes a monotonic function. At this time, the EMD decomposition will end and the original signal could be expressed as:

$$s(t) = \sum_{i=1}^{n} C_i + res \tag{2}$$

However, there are still some shortcomings in the EMD method. The main disadvantage is the Mode Mixing problem in the decomposition process. Mode Mixing refers to the phenomenon that an IMF component contains multiple signals of different frequencies, or the same frequency signal component is decomposed into different IMFs [9]. The discontinuity of the original signal frequency is the main cause of Mode Mixing. EMD decomposes signals in order of frequency from high to low. Due to the discontinuity of the signal frequency, when the decomposition of the high-frequency signal is imperfect, in order to satisfy the method, a part of the next frequency band is required to compensate for the missing portion of the high-frequency decomposition. This will cause the high-frequency component to become

a mixed component [9]. Therefore, in this case, the IMF component decomposed by the EMD method does not have a real physical meaning, thereby affecting subsequent signal processing.

EEMD was proposed to overcome the Mode Mixing of EMD. The EEMD algorithm inhibits Mode Mixing by utilizing the characteristics of a quasi-binary filter in the decomposition of Gaussian white noise [9]. That is, Gaussian white noise is added to the original signals, then the composite signals are decomposed by using EMD. And the noise in IMFs can be eliminated, so that original signals can be decomposed.

The procedural steps of EEMD are as follows [9]:

1) Initialize the number of loops N and the noise amplitude of the Gaussian white noise added to the signal, and let $i = 1$.
2) A Gaussian white noise $n_i(t)$ is added to the original signal $s(t)$ to form a new signal $s_i(t)$. $s_i(t)$ represents the new signal formed by adding the Gaussian white noise at the ith time, and $n_i(t)$ represents the ith Gaussian white noise, and the expression is as follows:

$$s_i(t) = s(t) + n_i(t) \quad (i = 1, 2, \cdots, N) \tag{3}$$

3) EMD decomposition is performed on the newly formed signal $s_i(t)$ to obtain n IMFs, and the result is as shown in the formula (4).

$$s_i(t) = \sum_{k=1}^{n} c_{i,k}(t) + r_{i,n}(t) \tag{4}$$

where, $c_{i,k}(t)$ is the obtained IMF component, $r_{i,n}(t)$ represents the residual component, and n represents the number of IMFs.

4) Repeat steps (1)-(3) for a total of N times, each time adding different Gaussian white noise of the same amplitude, and finally obtaining a set of IMFs:

$$\{\{c_{1,1}(t), c_{1,2}(t), \cdots, c_{1,n}(t)\}, \cdots, \{c_{N,1}(t), c_{N,2}(t), \cdots, c_{N,n}(t)\}\} \tag{5}$$

5) The mean value of the IMFs obtained by the N-time EMD method decomposition is calculated, and the average value is taken as the final result, and the calculation formula is as shown in the formula (6).

$$c_k(t) = \frac{\sum_{i=0}^{N} c_{i,k}(t)}{N} \ (i = 1, 2, \cdots, N; k = 1, 2, \cdots, n) \tag{6}$$

The decomposition process of the EEMD method is shown in the figure 2.

EEMD can inhibit Mode Mixing and accurately extract the features of vibration signals at the main frequency band. And the frequency structures of the OLTC vibration signal under different operating conditions are significantly different [2]. Thus, the vibration signal can be separated into Intrinsic Mode Functions (IMFs) of different frequency intervals by using EEMD, and the characteristics of mono-components can be extracted to realize the identification of mechanical faults.

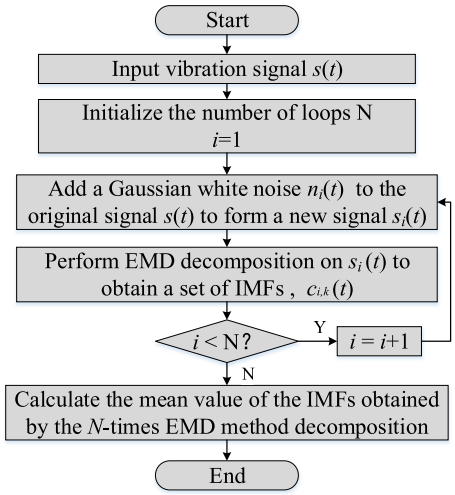

FIGURE 2. Flow chart of EEMD decomposition.

B. VOLTERRA MODEL FOR CHAOTIC TIME SERIES

The frequency structure of an IMF is not unitary, and its frequency is distributed in a range, thus it is not appropriate to use IMFs directly as characteristic parameters. Therefore, it is necessary to select appropriate methods to refine and simplify its feature information. The Volterra model for chaotic time series is a good solution. It could not only solve the non-stationary problem of signals but also greatly relieves the computational complexity and improves the computing speed [10].

The theory of phase-space reconstruction forms the basis for predicting chaotic time series. Takens [11] proposed phase-space reconstruction on chaotic time series $\{x(n)\}$ by applying delay coordinates. The mid-point of the phase space can be expressed as follows:

$$\boldsymbol{X}(\boldsymbol{n}) = \{x(n), x(n-\tau), \cdots, x[n-(m-1)\tau]\} \tag{7}$$

where, m and τ refer to the embedding dimension and time delay, respectively. Takens' theorem [11] shows that, when the embedding dimension $m \geq 2d + 1$ (d denotes the dimension of system dynamics), the reconstructed dynamic system is topologically equivalent to the original dynamic system. The chaotic attractors in the two-phase spaces show diffeomorphism. Therefore, it is feasible to attain the state at the next moment in time according to the current state of the system, thus acquiring the predicted value of a time series at the next moment [10]. Essentially, the prediction using a chaotic time series is an inverse problem of dynamic systems, that is, reconstructing the dynamic model $F[\boldsymbol{X}(\boldsymbol{n})]$ of the system according to the state of the dynamic system, namely,

$$x(n+T) = F[\boldsymbol{X}(\boldsymbol{n})] \tag{8}$$

where, T refers to the forward predictive step length ($T > 0$). There are many methods available for constructing a non-linear function to approach to $F[\boldsymbol{X}(\boldsymbol{n})]$. In this study, by using the Volterra series expansion [10], a non-linear prediction model $F[\boldsymbol{X}(\boldsymbol{n})]$ for a chaotic time series is established.

The input and output of the non-linear discrete system are set to $\boldsymbol{X}(\boldsymbol{n}) = \{x(n), x(n-\tau), \cdots, x[n-(m-1)\tau]\}$ and $y(n) = x(n+1)$. In this case, the Volterra series expansion for the function governing the non-linear system is as follows:

$$x(n+1) = h_0 + \sum_{k=1}^{p} y_k(n) \tag{9}$$

where,

$$y_k(n) = \sum_{i_1,\cdots,i_k=0}^{m-1} h_k(i_1,\cdots,i_k) \prod_{j=1}^{k} x\left(n - i_j\tau\right) \tag{10}$$

where, $h_k(i_1,\cdots,i_k)$ is called the k-order Volterra kernel and p represents the expansion order of the Volterra series. In practical application, it is hard to realise the expansion of the infinite series and therefore it is necessary to apply limited-order truncation and time-limited summation. For convenience of illustration, by taking second-order truncation and m summation operations as an example, the Volterra series expansion for predicting a chaotic time series is expressed as follows:

$$\begin{aligned} x(n+1) = h_0 &+ \sum_{i_1=0}^{m-1} h_1(i)\, x(n-i_1\tau) \\ &+ \sum_{i_1,i_2=0}^{m-1} h_k(i_1,i_2)\, x(n-i_1\tau)\, x(n-i_2\tau) \end{aligned} \tag{11}$$

The vectors of coefficients of Volterra series and input signals are separately displayed as follows:

$$\begin{aligned} \boldsymbol{W}(\boldsymbol{n}) = [&h_0, h_1(0), h_1(1), \cdots, \\ &h_1(m-1), h_2(0,0), h_2(0,1), \cdots, \\ &h_1(m-1, m-1)]^{\mathrm{T}} \end{aligned} \tag{12}$$

$$\begin{aligned} \boldsymbol{Z}(\boldsymbol{n}) = \{&1, x(n), x(n-\tau), \cdots, \\ &x[n-(m-1)\tau], x^2(n), x(n)\,x(n-\tau), \cdots, \\ &x^2[n-(m-1)\tau]\Big\}^{\mathrm{T}} \end{aligned} \tag{13}$$

Formula (7) can be expressed as follows:

$$x(n+1) = \boldsymbol{Z}^{\boldsymbol{T}}(\boldsymbol{n})\, \boldsymbol{W}(\boldsymbol{n}) \tag{14}$$

By using a normalised adaptive algorithm with least mean square residuals, the exact value of the coefficient vector$\boldsymbol{W}(\boldsymbol{n})$ can be obtained. Under this circumstance, $\boldsymbol{W}(\boldsymbol{n})$ contains important information characterising the state of the system [10].

The basic idea of extracting the characteristics of mechanical faults of an OLTC is summarised as follows: the mechanical vibration signals in the switchover process of the OLTC are decomposed by using EEMD. Afterwards, by utilising the Volterra series, various IMF components are expanded to form a matrix of coefficient vectors. Furthermore, the singular value of the matrix is calculated as the classification basis for diagnosing mechanical faults in the OLTC. The procedural steps are as follows:

1) The Volterra model for each IMF component is separately established and the coefficient vector $\boldsymbol{W}(\boldsymbol{n})$ of each model is calculated.

2) The coefficient vector of each Volterra model for IMF components is taken as lateral vector of the matrix to form a Volterra coefficient matrix.

3) The singular values of the Volterra coefficient matrix are calculated and taken as characteristic of the mechanical faults in the OLTC.

C. DECISION ACYCLIC GRAPH SUPPORT VECTOR MACHINE

In terms of pattern recognition, the widely used methods are artificial neural network (ANN) and support vector machine (SVM) model. ANN is composed of a large number of nonlinear neurons, so nonlinearity is its inevitable characteristic, and it has been successfully applied in many fields for its good nonlinear processing ability and effect [12]. Although the early theory of SVM is only applicable to linear processing, with the introduction of kernel function, SVM can map nonlinear input samples to high-dimensional feature space, which greatly enhances the nonlinear processing ability of SVM [13]. ANN has strong learning ability, easy to realize parallel computing, and also has good adaptive ability and fault tolerance. However, the network structure of ANN is difficult to determine [14]. If it is not selected properly, problems such as over-fitting or under-learning will occur. For example, if the initial value of the network is set differently, the network structure and effect will also be different. In comparison, the system structure of SVM is relatively simple. Although the structure of SVM is similar to three-layer BP ANN, the hidden layer of SVM can be determined automatically by the algorithm, and the scale of the system can be adjusted adaptively [13]. Therefore, SVM does not have the problem of structure determination like ANN and does not need too much prior knowledge. In the processing of small sample data, ANN has poor learning effect. However, SVM is a machine learning method based on small samples, whose computation is almost irrelevant to the sample dimension, which is more suitable for solving many practical problems [13]. In the field of diagnosing mechanical faults in OLTC, different OLTCs have differences in working principle, mechanical structure and voltage level, so trained SVM or ANN of a specific OLTC may not be well applicable to other OLTCs. Therefore, whether to use SVM or ANN, if you want to diagnose a mechanical fault of a certain type of OLTC, it is necessary to obtain OLTC's actual vibration data for training. However, OLTC is affected by operating procedures, so the number of actions is limited in a certain period of time [15]. In this case, it is difficult to obtain a

large amount of data of the same working condition during its operation. This puts a high demand on the model's ability to process small sample data. In a word, although which of SVM and ANN are more advanced is still inconclusive, SVM is obviously more suitable for diagnosing mechanical faults of OLTC.

The idea of using an SVM to solve classification problems is to search for an optimal hyperplane which can satisfy the classification requirement. On the condition of satisfying the classification accuracy of the optimal hyperplane, it needs to guarantee a blank space at the two sides of the hyperplane to be a maximum [16]. The method can solve non-linear problems and theoretically realise the optimal classification of linearly separated data. Mechanical faults on an OLTC are generally few in number, and the SVM shows excellent performance in classification of small sample data, so it was applied here as the classification method [17].

However, SVM has an obvious disadvantage compared to ANN. That is, SVM was originally proposed for binary classification problems and cannot be directly used to solve multivariate classification problems [18]. However, the fault diagnosis problem of OLTC is multivariate classification, so how to effectively extend SVM to multivariate classification is an urgent problem to be solved. At present, there are two main solutions for multi-classification SVM [18]: one is to directly establish multi-objective classification function solution, which uses more variables and the computational complexity is too high; the second is to transform the multi-classification problem into multiple binary classification problems, mainly including voting method, hierarchical method and Directed Acyclic Graph Support Vector Machine (DAG-SVM) methods . And the first two methods have poor performance in some aspects such as rejection blind zone and sample balance, so it is necessary to develop DAG-SVM diagnostic methods. DAG-SVM combines the sample balance of SVM and the feature of the hierarchical classifier without blind spots, so it is widely used in the current diagnostic methods [16].

The DAG-SVM is a multi-classification expansion strategy, which can relieve asymmetry in samples, optimises training and decision-making times [16]. The strategy is proposed on the basis of a decision directed acyclic graph (common in graph theory) during the decision phase. For the classification problem, the DAG-SVM uses $k(k\text{-}1)/2$ SVMs to exclude impossible classification results layer by layer. Finally, the final classification result can be obtained. Because each classifier corresponds to two types of samples, it has better sample balance and thus has better classification effect [18]. On the condition of not increasing the computational burden during decision-making, the DAG-SVM chooses different decision-making paths for different data, thus improving partitioning accuracy. By taking four-classification problem as an example, the decision-making structure of the DAG-SVM is as shown in figure 3. Where i denotes the working condition category of OLTC, $i = 1, 2, 3, 4$; 1-vs-4 denotes the SVM model trained by the category 1 and category 4 training data.

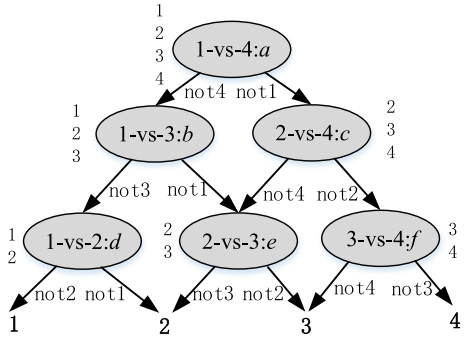

FIGURE 3. Diagnostic process of four-classification DAG-SVM. It is composed of 6 binary classification SVM based on decision directed acyclic graph.

a. The SYJZZ-35 OLTC b. The experiment platform

FIGURE 4. The SYJZZ-35 OLTC and the experiment platform. SYJZZ-35 is an experimental model for simulating OLTC mechanical faults. The experimental platform consists of SYJZZ-35 and data acquisition system.

The top layer contains only one node, called the root node, the second layer contains 2 nodes, and so on, and the Nth layer contains only N nodes.

The following are examples of the data classification process of DAG-SVM: For input sample X whose category is 4, X will go through the 3 nodes: *a-c-f*, and finally be classified into category 4; if the given category of X is 3, X will pass through the three nodes: *a-c-e or a-b-e or a-c-f*, and finally divided into category 3.

III. TEST EXPERIMENT FOR ON-LOAG TAP CHANGER MECHANICAL FAULTS

A. THE EXPERIMENTAL ON-LOAG TAP CHANGER

In the present study, an SYJZZ-35 OLTC was used: with an embedded composite resistance-type transition structure, the SYJZZ-35 OLTC can integrate the functions of tap selector and switch. The core of the switch and the electrical mechanism are designed as an integrated plug-in structure. It can be installed in a single oil cavity isolated from the transformer (figure 4).

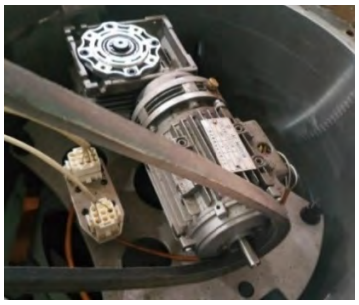

FIGURE 5. Simulating a motor jam fault inSYJZZ-35 OLTC.

The three-phase SYJZZ-35 OLTC adopts jumper voltage regulation at the middle part, with the rated voltage of 35 kV, resistance transition, direct switching, and seven working positions. Moreover, with the simple structure, this type of OLTC has a long service life, and it is easy to disassemble and maintain, making it fit for purpose.

B. TESTING OF TYPICAL MECHANICAL FAULTS ON THE ON-LOAG TAP CHANGER

To validate the effectiveness of the new time-frequency vibration analysis, the loosening and jamming faults (including loosening of moving and transition contacts as well as motor jamming) were simulated. Owing to loosening and jamming faults accounting for more than 60% of all faults, these faults were a good representation. Existing test and operational experience showed that early mechanical faults of the OLTC were difficult to detect through existing monitoring of quantities including current and rotation angle. In this experiment, the loosening can be simulated by partly removing fastening screws or springs, and motor jamming was simulated by applying resistance to the motor shaft (figure 5, figure 6).

Figure 7 shows the schematic diagram of the test system, which includes:

① OLTC Automatic controller: It can issue commands to the OLTC to enable the OLTC to complete voltage and gear adjustments;

② SYJZZ-35 OLTC: The most important part of the test platform, which can simulate the mechanical faults and generate vibration signals during the switching process;

③ UTL2001X piezoelectricity acceleration sensors: It is used to detect vibrations from the OLTC;

④ The signal conditioning module: It can process the vibration signal by amplification, isolation, filtering, denoising, etc. Therefore, noise interference can be removed.

⑤ DATAQ DI-4108 data acquisition system: It can transform the analogy signal into a digital signal. Its sampling frequency is 50 kHz.

⑥ Computer: Data logging and data processing

Three UTL2001X piezoelectricity acceleration sensors (sensitivity: 500 mV/g, Nos 1∼3) produced by Quatech Electronic Company Ltd (Beijing, China) were used in the experiment. By applying a DI-4108 data acquisition system (DATAQ Company Ltd, USA) the vibration signals in the

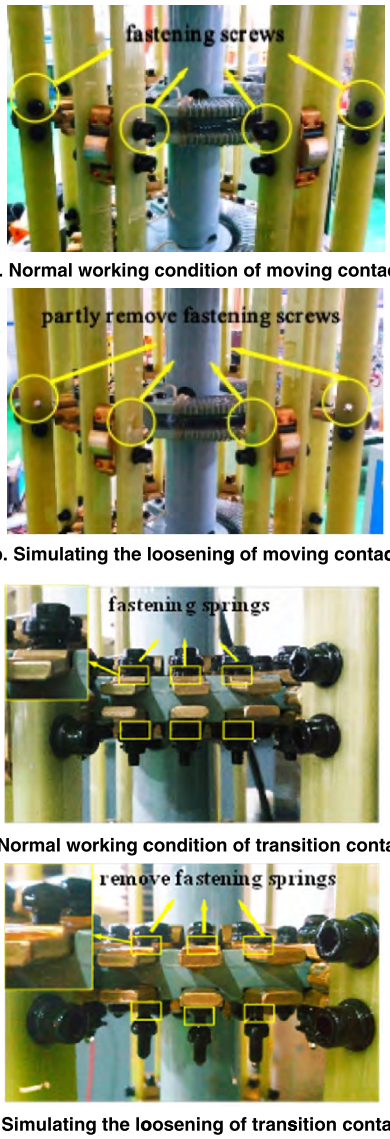

FIGURE 6. Simulating a typical loosening fault in SYJZZ-35 OLTC.

switchover process of the OLTC were tested. Based on practical experience, to reduce the interference of vibration signals from transformers during operation and for convenience of installation, the three sensors were separately distributed on the top and two flanks of the wall of the transformer tank. In this way, it was convenient to acquire mechanical vibration signals in three different orthogonal directions in the switchover process of the OLTC, as shown in figure 8.

The steps for data acquisition are as follows:

1) Adjusting the OLTC automatic controller to send an action instruction to the OLTC;
2) The OLTC performs gear shifting to generate a vibration signal;
3) The piezoelectricity acceleration sensors on the surface of the OLTC receives the vibration signal and sends it to the signal conditioning module;

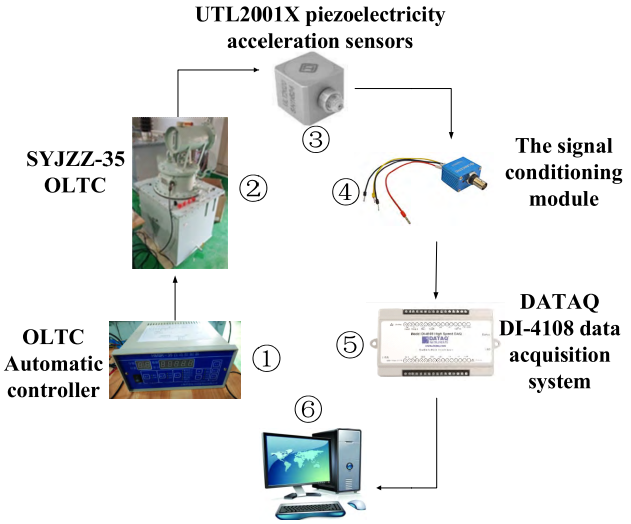

FIGURE 7. Schematic diagram of the experimental platform. This figure shows the composition and connection of the experimental platform (figure 4b).

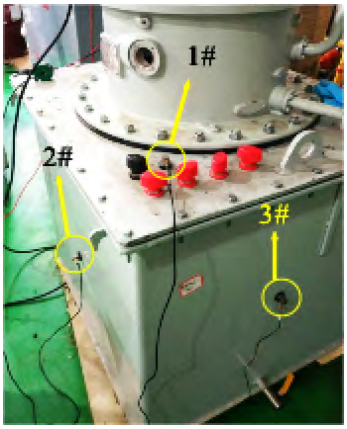

FIGURE 8. Positions of the piezoelectricity acceleration sensors. Three sensors collect vibration signals in three directions of X, Y and Z axes.

4) The signal conditioning module processes the vibration signal by amplification, isolation, filtering, denoising, etc., and then sends the signal to the data acquisition system;
5) The data acquisition system transforms the analogy signal into a digital signal and sends it to the software on the computer for recording and processing.

Additionally, to verify the consistency of the switchover process of the OLTC and eliminate the influence of random error on the test result, a full tap position test was conducted. The OLTC was switched over from the first tap position to the seventh tap position (uplink) and then reverse-switched over to the first tap position (downlink), and this cycle repeated nine times. For each type of fault, 108 groups of data were acquired, in which 54 groups of data separately corresponded to odd-even and even-odd shifts. Additionally, for the loosening of contacts, the contacts in each of the three phases of the OLTC were all simulated by considering the influence of different fault positions on the collected vibration signals.

IV. EXPERIMENTAL ANALYSIS

A. ENSEMBLE EMPIRICAL MODE DECOMPOSITION

At first, the vibration signals in the switchover process of the OLTC under normal working conditions were analysed. Figure 9 displays the vibration signals measured at three points in a switchover process and IMFs obtained by using EEMD (limited by word-count, only IMF1 to IMF4 are shown). The vibration signals were all time-variant and non-stationary. Figure 10 displays general spectrums for vibration signals under four working conditions:

1) Under normal working condition, the frequency of the OLTC vibration signal is mainly concentrated within 2500 Hz;
2) Under moving contact loosening condition, the low frequency part and the frequency within 2500 Hz - 6000 Hz will be significantly enhanced compared with the normal working condition;
3) Under transition contact loosening condition, the low frequency part has no obvious change compared with the normal working condition, but the frequency component around 2500 Hz will increase significantly;
4) Under motor jamming condition, the frequency components below 5000 Hz will increase significantly compared with the normal working condition.

In summary, the frequency structure of the OLTC vibration signal under different working conditions will be significantly different. Therefore, it is feasible to diagnose typical mechanical faults of OLTC by performing frequency domain analysis on OLTC vibration signals. EEMD can separate the vibration signal into mono-components (IMFs) of different frequency intervals, then the characteristics of mono-components can be quantified by Volterra model to realize the identification of mechanical faults.

Figure 11 shows the Hilbert marginal spectrums of IMF1 to IMF3 (normal working condition) obtained by using the traditional EMD and the EEMD. The magnitude of the Hilbert marginal spectrum represents the sum of the amplitudes of a certain frequency in a signal at various times [11]. As shown in figure 11, the IMF2 obtained by using EMD had exhibited Mode Mixing. While, by using EEMD, possible Mode Mixing could be effectively inhibited. Therefore, various narrow-band frequency components contained in vibration signals can be independently distributed in various IMFs

B. OBTAINING FAULT FEATURES BASED ON THE VOLTERRA MODEL

In the previous process, the vibration signal has been decomposed into IMFs by using EEMD. Figure 9 shows that the IMF4 component contained less information. Therefore, IMF1 to IMF4, with a majority of the characteristics of the OLTC therein, were used in next steps. Each IMF could establish a Volterra model. As discussed in Section 1.2, a finite truncation of the Volterra series would be performed and a coefficient vector could be formed by the coefficients of the first 10 terms. Furthermore, the coefficient vector corresponding to each IMF could be seemed as a row of a

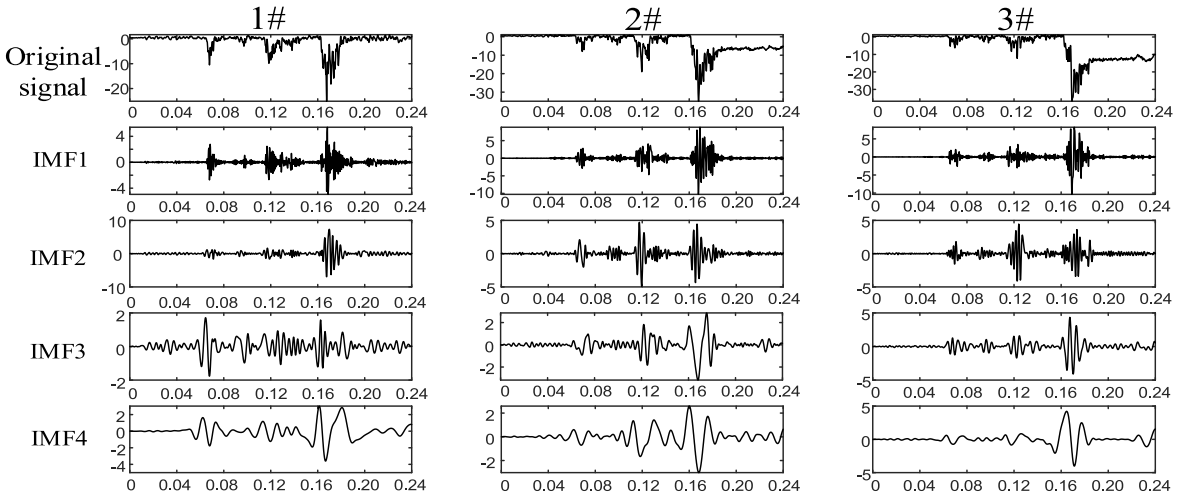

FIGURE 9. The original vibration signals measured by the piezoelectricity acceleration sensors and the IMF1-IMF4 obtained by EEMD decomposition.

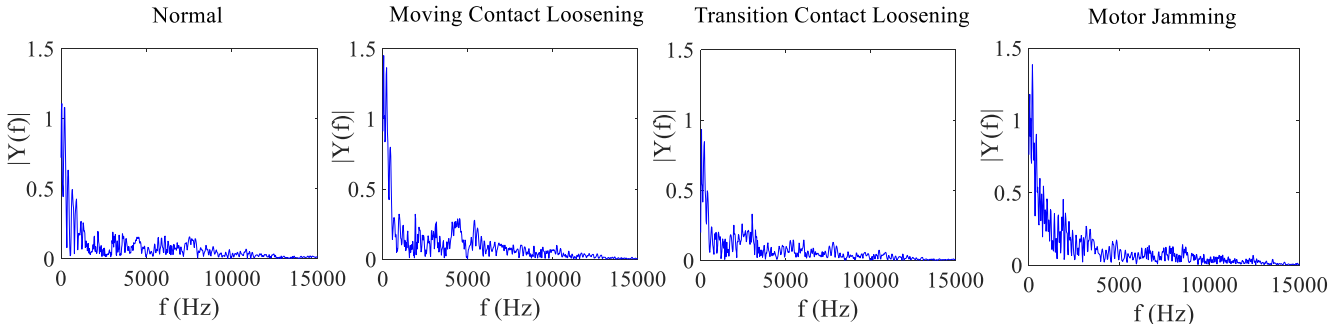

FIGURE 10. General spectrums for vibration signals under different working conditions.

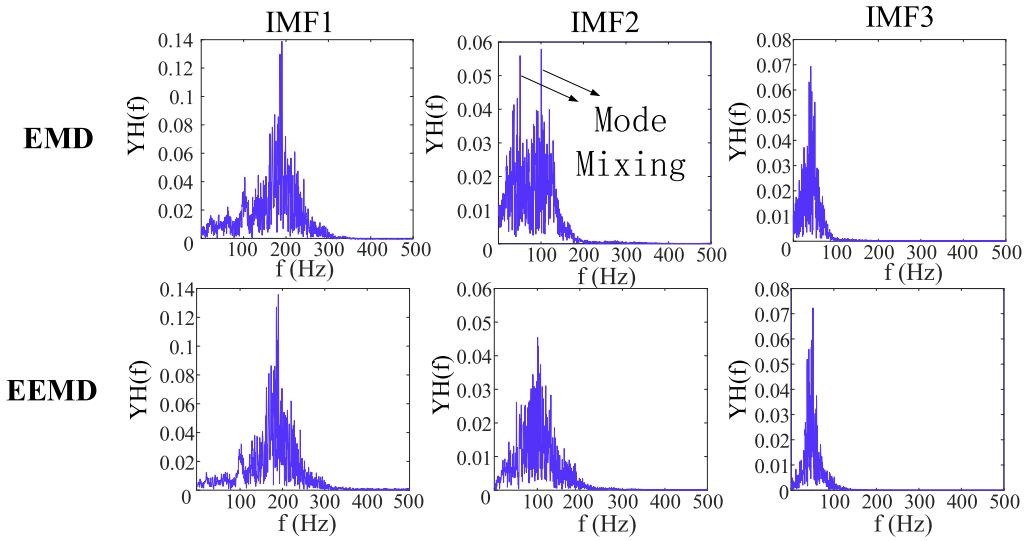

FIGURE 11. Hilbert marginal spectrums of IMFs obtained by using EMD and EEMD (Normal Working Condition).

matrix. So, a matrix of 12×10 could be built based on 12 coefficient vectors, which is the Volterra coefficient matrix. It characterizes the information contained in the vibration signal during an OLTC switching process.

It is worth noting that the embedded dimension $m = 3$ of the Volterra model for a chaotic time series can be solved by using Cao's method [17] while the delay time $r = 1$ was calculated by applying mutually available information [19].

TABLE 1. Volterra coefficient matrix under normal working conditions.

Measuring point 1(1#)										
IMF1	-0.0014	1.3253	-0.2217	-1.1912	0.0730	0.5349	0.4267	0.1381	0.1229	-0.2834
IMF2	-0.0007	1.1836	0.0334	0.1179	0.0604	0.0206	-0.5356	0.1014	0.0040	-0.0664
IMF3	0.0001	1.3053	0.0098	0.2291	-0.0011	-0.0097	-0.6151	-0.0023	-0.0068	0.0010
IMF4	-0.0001	1.2277	-0.0031	0.3268	0.0019	-0.0011	-0.5668	0.0113	0.0004	-0.0059
Measuring point 2(2#)										
IMF1	-0.0001	1.4882	-0.3174	-1.0692	-0.0855	0.2064	0.1718	0.0015	0.1107	0.1856
IMF2	0.0001	1.2968	0.0011	0.0126	0.0107	0.0192	-0.5276	-0.0117	-0.0046	-0.0201
IMF3	0.0003	1.3007	-0.0040	0.2884	-0.0023	-0.0019	-0.6282	-0.0021	-0.0034	-0.0069
IMF4	0.0000	1.1776	-0.0035	0.3284	-0.0020	-0.0007	-0.5177	-0.0006	0.0005	0.0016
Measuring point 3(3#)										
IMF1	-0.0004	1.4663	0.3939	-0.9813	0.1061	-0.1220	0.1729	-0.1733	-0.2153	-0.1792
IMF2	-0.0008	1.2547	-0.0470	-0.1104	0.0272	0.0002	-0.4435	0.1727	0.0442	-0.0398
IMF3	0.0001	1.2797	-0.0219	0.2874	-0.0137	0.0026	-0.6552	-0.0142	0.0095	0.0237
IMF4	-0.0002	1.1191	-0.0157	0.3286	-0.0049	0.0009	-0.4598	0.0083	0.0094	0.0132

TABLE 2. SVD result under normal working conditions.

Measuring Point No. \ Sample No.	1	2	3	4	5
1#	2.610	2.610	2.606	2.602	2.593
	1.277	1.322	1.292	1.278	1.429
	0.317	0.194	0.153	0.282	0.188
	0.074	0.078	0.085	0.090	0.107
2#	2.628	2.589	2.643	2.668	2.643
	1.427	1.346	1.421	1.453	1.352
	0.368	0.118	0.181	0.168	0.143
	0.067	0.037	0.141	0.052	0.050
3#	2.692	2.690	2.694	2.702	2.542
	1.599	1.313	1.347	1.214	0.994
	0.270	0.323	0.085	0.147	0.275
	0.025	0.090	0.040	0.025	0.038

TABLE 3. SVD result under moving contact loosening conditions.

Measuring Point No. \ Sample No.	1	2	3	4	5
1#	2.826	2.835	2.815	2.838	2.840
	1.310	1.619	1.573	1.406	1.832
	0.183	0.184	0.102	0.319	0.118
	0.084	0.039	0.029	0.022	0.027
2#	2.650	2.697	2.666	2.646	2.704
	1.186	1.252	1.648	1.510	1.617
	0.169	0.192	0.114	0.175	0.226
	0.126	0.093	0.013	0.085	0.046
3#	2.595	2.717	2.664	2.739	2.798
	1.455	1.482	1.486	1.418	1.476
	0.173	0.131	0.175	0.103	0.246
	0.027	0.034	0.051	0.040	0.035

TABLE 4. SVD result under transition contact loosening conditions.

Measuring Point No. \ Sample No.	1	2	3	4	5
1#	2.718	2.737	2.724	2.703	2.729
	1.228	1.376	1.673	1.604	1.318
	0.223	0.297	0.180	0.149	0.226
	0.057	0.032	0.046	0.079	0.080
2#	2.754	2.766	2.723	2.757	2.712
	1.480	1.554	1.610	1.561	1.590
	0.182	0.223	0.125	0.319	0.190
	0.024	0.031	0.044	0.040	0.096
3#	2.676	2.747	2.765	2.684	2.768
	1.421	1.410	1.327	1.285	1.277
	0.282	0.476	0.112	0.277	0.278
	0.011	0.013	0.030	0.107	0.019

TABLE 5. SVD result under motor jamming conditions.

Measuring Point No. \ Sample No.	1	2	3	4	5
1#	2.938	2.966	2.918	2.930	2.985
	1.413	1.695	1.546	1.584	1.728
	0.445	0.205	0.261	0.175	0.253
	0.041	0.048	0.055	0.082	0.063
2#	2.684	2.672	2.680	2.612	2.676
	1.628	1.544	1.405	1.478	1.555
	0.158	0.211	0.310	0.107	0.146
	0.054	0.054	0.072	0.020	0.063
3#	2.588	2.658	2.776	2.691	2.668
	1.430	1.450	1.187	1.418	1.328
	0.351	0.228	0.111	0.204	0.215
	0.075	0.065	0.043	0.045	0.054

The expansion order of the Volterra series was two. For example, table 1 shows the Volterra coefficient matrix under normal operating conditions obtained by using EEMD and Volterra model.

Table 2 to table 5 list the singular values obtained through singular value decomposition (SVD) of the Volterra coefficient matrix in various working conditions. Limited by word-count, only five groups of samples from each working condition are displayed. Each group of singular values corresponds to a vibration signal during the OLTC switching process. The singular values in table 2 to table 5 could be used as characteristic parameters for judging the mechanical state of the OLTC.

As shown in table 2 to table 5, the SVD results of the OLTC in different mechanical states presented significant regularity at monitoring point 1 while the singular values at other monitoring points varied. This can be easily explained from the perspective of the model structure and the positions of monitoring points during the experiment. The tap positions of SYJZZ-35 OLTCs were switched over by rotation, however, due to the requirements of non-intrusive detection, the sensors cannot enter the interior of the transformer but

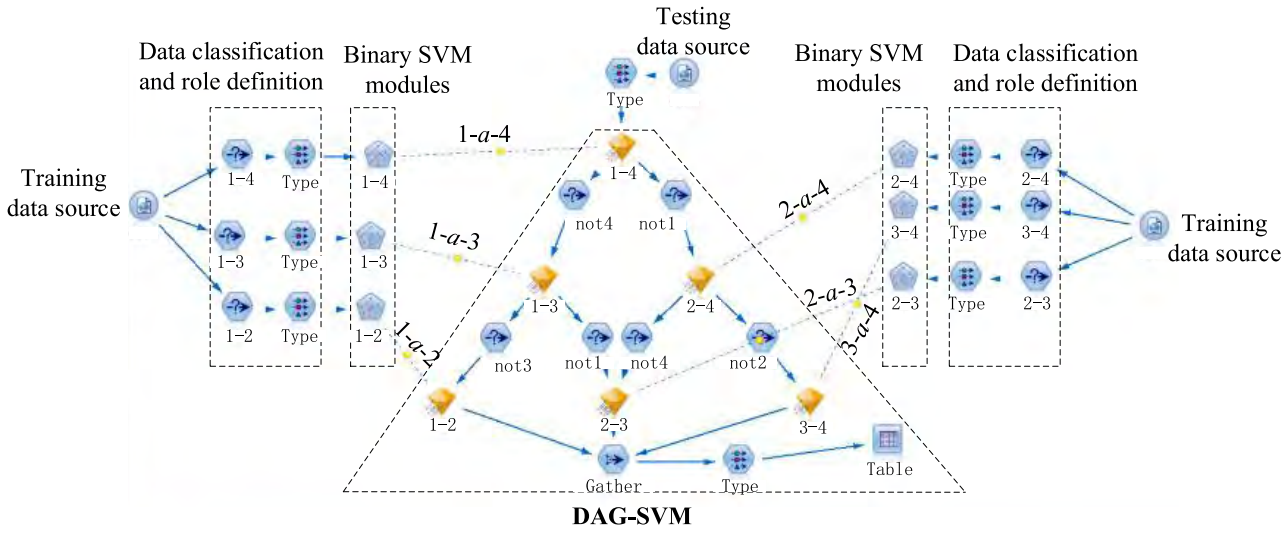

FIGURE 12. Four-classification DAG-SVM model. This model was built in IBM SPSS Modeler according to the principle shown in figure 3.

were only installed on the wall of the tank. This meant that, during the full tap position switchover experiment, the vibration signals collected by the two sensors at the flanks of the tank were influenced by the tap switchover positions; however, monitoring point 1 was located on the top of the tank and therefore was not significantly influenced. That is, except for monitoring point 1, the trend of the singular values at the other monitored points were difficult to explore by using the observational method. Thus, it is necessary to apply SVMs. Through much data training, the SVM can realise an intellectualised output of decisions, classify and predict data. It can avoid the misjudgement caused by subjective experience of maintenance engineers, showing high accuracy and reliability.

C. IDENTIFYING MECHANICAL FAULTS ON OLTC USING THE DECISION ACYCLIC GRAPH SUPPORT VECTOR MACHINE

A DAG-SVM classification model was established by using specialised data mining tool IBM SPSS Modeler. In one switch process, 12 singular values (each measurement point corresponds to 4 singular values) can be obtained by using EEMD, Volterra model and SVD. They were used as decision variables for SVM classification. Meanwhile, the mechanical working condition was taken as an object variable. Working conditions were labelled: normal working condition–1, loosening of moving contact–2, loosening of transition contact–3, and motor jam–4. Taking the diagnostic process inherent to DAG-SVM (figure 3), positive and negative sample sets for each two-classification SVM could be determined. By employing IBM SPSS Modeler, a four-classification DAG-SVM model was established (figure 12).

The singular values of Volterra coefficient matrix could be imported into the data source module, which could be used to train binary SVM modules. According to the DAG-SVM construction method, these binary SVM modules can constitute a multi-classification SVM model to classify and identify various typical mechanical faults in an OLTC.

The singular values of the Volterra coefficient matrix would be obtained by the new method. 432 sets of data were used in in the process of building the DAG-SVM model. Among them, 108 sets of normal working conditions, 108 sets of moving contact loosening conditions, 108 sets of transition contact loosening conditions, and 108 sets of motor jamming conditions. And they were divided in terms of training (60%), validation (20%) and test (20%) sets. According to the operating experience of STATE GRID Corporation of China, the on-load tap-changer is switched about 2,000 times in 2 years [15]. Once it had been running for half a year or one year, it should be dismantled and repaired according to the operating specifications [15]. The fault diagnosis method analysis method proposed in this paper aims to eliminate the mechanical hidden danger of the on-load tap-changer, and the vibration waveform of the same mechanical fault is extremely similar, so the number of data sets is sufficiently representative.

According to the classification of DAG-SVM model, the fault category and tendency score of each data group could be obtained (table 6).

In table 6, X01-X12 represents the 12 singular values obtained by the singular value decomposition (SVD) of the Volterra coefficient matrix. Among them, the vibration signal of each measurement point is processed to obtain 4 singular values (1#: X01-X04, 2#: X05-X08, 3#: X09-X12); ''Actual Condition'' indicates the actual mechanical fault type corresponding to the set of singular values (normal working condition–1, loosening of moving contact–2, loosening of transition contact–3, and motor jam–4) and ''Model Judgment'' represents the judgment result of the DAG-SVM model; The classification result obtained by the support

TABLE 6. Diagnostic results of mechanical states of the OLTC based on experimental data.

Sample No.	SVD results												Actual condition	Model judgment	Tendency score
	X01	X02	X03	X04	X05	X06	X07	X08	X09	X10	X11	X12			
1	2.703	1.604	0.149	0.079	2.757	1.561	0.319	0.040	2.684	1.285	0.277	0.106	3	3	0.857
2	2.938	1.413	0.445	0.041	2.684	1.628	0.158	0.054	2.588	1.430	0.351	0.075	4	4	0.856
3	2.966	1.695	0.205	0.048	2.672	1.544	0.211	0.054	2.658	1.450	0.228	0.065	4	4	0.856
4	2.918	1.546	0.261	0.055	2.680	1.405	0.310	0.072	2.776	1.187	0.111	0.043	4	4	0.856
5	2.929	1.584	0.175	0.082	2.612	1.478	0.107	0.020	2.691	1.418	0.204	0.045	4	4	0.856
6	2.985	1.728	0.253	0.063	2.676	1.555	0.146	0.063	2.668	1.328	0.215	0.054	4	4	0.862
7	2.835	1.619	0.184	0.039	2.696	1.252	0.192	0.093	2.717	1.482	0.131	0.034	2	2	0.867
8	2.814	1.573	0.102	0.029	2.666	1.648	0.114	0.013	2.664	1.486	0.175	0.051	2	2	0.855
9	2.837	1.406	0.319	0.022	2.646	1.510	0.175	0.085	2.739	1.418	0.103	0.040	2	2	0.855
10	2.840	1.832	0.118	0.027	2.704	1.617	0.226	0.046	2.798	1.476	0.246	0.035	2	2	0.855
11	2.737	1.376	0.297	0.032	2.766	1.554	0.223	0.031	2.747	1.410	0.476	0.013	3	3	0.853
12	2.724	1.673	0.180	0.046	2.723	1.610	0.125	0.043	2.765	1.327	0.112	0.030	3	3	0.853
13	2.610	1.277	0.317	0.074	2.628	1.427	0.368	0.067	2.692	1.599	0.270	0.025	1	1	0.856
14	2.610	1.322	0.194	0.077	2.589	1.346	0.118	0.037	2.689	1.313	0.323	0.090	1	1	0.856
15	2.606	1.292	0.153	0.085	2.643	1.421	0.181	0.141	2.694	1.347	0.085	0.040	1	1	0.856
16	2.602	1.278	0.282	0.090	2.668	1.453	0.168	0.052	2.702	1.214	0.147	0.025	1	1	0.856
17	2.593	1.429	0.188	0.107	2.643	1.352	0.143	0.050	2.542	0.994	0.275	0.037	1	1	0.856
18	2.703	1.604	0.149	0.079	2.757	1.561	0.319	0.040	2.684	1.285	0.277	0.106	3	3	0.857
19	2.938	1.413	0.445	0.041	2.684	1.628	0.158	0.054	2.588	1.430	0.351	0.075	4	4	0.856
20	2.966	1.695	0.205	0.048	2.672	1.544	0.211	0.054	2.658	1.450	0.228	0.065	4	4	0.856

vector machine is a prediction result and it is not completely determined. ''Tendency score'' in table 6 indicates the possibility of this prediction result being correct. Its value is between 0.0 and 1.0. The higher the value, the higher the accuracy of the prediction result. Table 6 shows that for the 20 sets of verification data, the diagnostic results obtained by the new method proposed in this paper are consistent with the actual situation. Moreover, the ''tendency score'' index of each group of data is greater than or equal to 0.85, which indicates that the judgment result of the fault diagnosis model of this paper has high accuracy.

The experimental results revealed that the model for data diagnosis used in this study can detect typical mechanical faults in an OLTC with high accuracy.

To verify the effectiveness and accuracy of the proposed feature extraction method, different feature extractions was conducted, involving Wavelet Packet Decomposition (WPD) [6], EMD [1], EEMD [2], and EEMD-Volterra. Moreover, by applying the DAG-SVM [16] model, a comparison was made of the extraction efficacy of different methods. By checking 200 sets of vibration data in the switchover process of the OLTC under different working conditions, the accuracies of the four feature extraction methods are as listed in table 7.

According to table 7, compared with the other feature extraction method methods, the EEMD-Volterra method proposed in the paper showed a higher accuracy (at the same time, the analysis above could be verified).

To verify the effectiveness and accuracy of the proposed pattern recognition method, this paper presents the confusion matrices [20] of SVM [13], ANN [12] and DAG-SVM [16]

TABLE 7. Accuracies of different methods for fault diagnosis (OBTAINED by checking 200 sets of vibration data).

Method	Correctly identified	Misidentified	Correct rate
WPD	170	30	85.0%
EMD	187	13	93.5%
EEMD	191	9	95.5%
EEMD-Volterra	197	3	98.5%

to compare the classification accuracy of the three methods. The feature extraction method all used the EEMD-Volterra. Both SVM and DAG-SVM used Radial Basis Function (RBF) kernel [22]. RBF neural network [23] is a kind of feedforward neural network. It can approximate arbitrary nonlinear functions with arbitrary precision and has global approximation ability, which fundamentally solves the local optimal problem of Back Propagation (BP) neural network [23]. Therefore, the RBF neural network is compared with SVM and DAG-SVM as a representative of ANNs. By checking 200 sets of vibration data in the switchover process of the OLTC under different working conditions, the confusion matrices of the three pattern recognition methods are as listed in table 8 to table 10.

The statistical analysis results of the classification of the three pattern recognition methods are shown in Table 11. The ''Kappa'' coefficient is another measure of the accuracy of the classification, which indicates the degree of fit between the predicted condition and the true condition, and it is a more accurate evaluation index of the objective [21]. The formula

TABLE 8. Confusion matrix of SVM with RBF kernel (obtained by checking 200 sets of vibration data).

		Predicted condition			
		1	2	3	4
True condition	1	50	0	0	0
	2	0	27	11	12
	3	0	11	29	10
	4	0	12	13	25

TABLE 9. Confusion matrix of RBF neural network (obtained by checking 200 sets of vibration data).

		Predicted condition			
		1	2	3	4
True condition	1	47	2	0	1
	2	2	45	2	1
	3	1	1	46	2
	4	2	3	1	44

TABLE 10. Confusion matrix of DAG-SVM with RBF kernel (obtained by checking 200 sets of vibration data).

		Predicted condition			
		1	2	3	4
True condition	1	50	0	0	0
	2	0	48	2	0
	3	0	1	49	0
	4	0	0	0	50

TABLE 11. Statistical results of classification accuracy of three pattern recognition methods.

Method	Correctly identified	Correct rate	Kappa
SVM	131/200	65.5%	0.452
ANN	182/200	91.0%	0.827
DAG-SVM	197/200	98.5%	0.958

is as follows:

$$Kappa = \frac{N\sum_{i=0}^{c-1} a_{ii} - \sum_{i=0}^{c-1}(a_{i+}a_{+i})}{N^2 - \sum_{i=0}^{c-1}(a_{i+}a_{+i})} \quad (15)$$

where, a_{ii} represents the value on the diagonal of the confusing matrix; a_{i+}, a_{+i} respectively represent the sum of the ith row of the confusing matrix and the sum of the jth column; N is the total number of test samples.

In Section II, Part C, this article has compared SVM, ANN and DAG-SVM in detail, and pointed out the superiority of DAG-SVM compared to the other two methods, which can be verified here. Due to the weak multi-classification capability of the SVM [18], it obtained the worst classification result. ANN has the multiple classification capability, so it has higher classification accuracy than SVM, but it is limited by the number of samples and did not achieve the best result [13].

TABLE 12. Statistical results of classification accuracy of three pattern recognition methods with different kernel.

Method	Kernel	Correctly identified	Correct rate	Kappa
ANN	BP network	173/200	86.5%	0.775
	RBF network	182/200	91.0%	0.827
SVM	Linear Kernel	117/200	58.5%	0.407
	Polynomial Kernel	131/200	64.0%	0.429
	RBF Kernel	128/200	65.5%	0.452
DAG-SVM	Linear Kernel	188/200	94.0%	0.911
	Polynomial Kernel	197/200	96.0%	0.932
	RBF Kernel	192/200	98.5%	0.958

DAG-SVM is a multi-classification extension of SVM. It has strong multi-classification ability [18] and can process small sample data well [13], thus achieving the best classification effect.

Transform the kernel functions [22] of SVM and DAG-SVM, use the same method to obtain the confusion matrices and calculate the classification accuracy. The statistical results are shown in Table 12. At the same time, the classification accuracies of RBF neural network and BP neural network [23] are also listed in the table.

It can be seen from Table 12 that the DAG-SVM algorithm with RBF Kernel has the highest classification accuracy for the pattern recognition of OLTC mechanical fault types and it is most suitable for the diagnosis of OLTC mechanical faults.

V. CONCLUSIONS

A Method based on EEMD-Volterra and DAG-SVM was proposed for diagnosing mechanical faults in an OLTC. By using the EEMD-Volterra method, the features of vibration signals in the switchover process of OLTC were extracted. Meanwhile a DAG-SVM classification model for classification and fitting was established based on IBM SPSS Modeler, expecting to partition the automatic classification of mechanical states of the OLTC in an intelligent manner. The method can overcome issues related to fuzziness, complexity, and nonlinearity of the diagnosis of mechanical faults in an OLTC.

1) The EEMD algorithm can extract features from vibration signals at the main frequency band and inhibit possible Mode Mixing, thus improving the accuracy of decomposition of vibration signals of the OLTC.

2) The Volterra model for chaotic time series could not only solve the non-stationary problem of signals but also greatly relieves the computational complexity and improves the computing speed.

3) By using IBM SPSS Modeller, an intelligent multi-classification fitting model DAG-SVM was established to produce intellectualised output of decisions and intuitively classify and predict the data.

4) The experimental results showed that the method proposed could detect typical mechanical faults in an OLTC, showing a higher accuracy than other existing methods.

In conclusion, the effectiveness and practicability of the proposed method for diagnosing mechanical faults of OLTC were fully validated. Furthermore, it is necessary to simulate and analyse more faults, so as to improve the database of features of mechanical states of OLTCs. It is expected to provide a theoretical basis and practical guidance for on-line monitoring and fault diagnosis in an OLTC.

APPENDIX

TABLE 13. The abbreviation table.

Term	Abbreviation
Artificial Neural Network	ANN
Back Propagation	BP
Decision Acyclic Graph Support Vector Machine	DAG-SVM
Empirical Mode Decomposition	EMD
Ensemble Empirical Mode Decomposition	EEMD
narrowband noise-assisted multivariable EMD	NA-MEMD
Genetic Algorithm	GA
Intrinsic Mode Function	IMF
On-load Tap Changer	OLTC
On-load Tap Changing Transformer	OLTCT
Radial Basis Function	RBF
Support Vector Machine	SVM
Wavelet Packet Decomposition	WPD

REFERENCES

[1] Z. Li, Q. Li, Z. Wu, J. Yu, and R. Zheng, "A fault diagnosis method for on load tap changer of aerospace power grid based on the current detection," *IEEE Access*, vol. 6, pp. 24148–24156, 2018.
[2] R. Duan and F. Wang, " Fault diagnosis of on-load tap-changer in converter transformer based on time–frequency vibration analysis," *IEEE Trans. Ind. Electron.*, vol. 63, no. 6, pp. 3815–3823, Jun. 2016.
[3] Q. Li, T. Zhao, L. Zhang, and J. Lou, "Mechanical fault diagnostics of onload tap changer within power transformers based on hidden Markov model," *IEEE Trans. Power Del.*, vol. 27, no. 2, pp. 596–601, Apr. 2012.
[4] N. Saravanakumar and K. Sathiyasekar, "Circular array of ultrasonic sensor based DOA estimation: Location of multiple partial discharge in transformer oil," *J. Electromagn. Waves Appl.*, vol. 32, no. 12, pp. 1569–1585, Aug. 2018.
[5] P. Kang and D. Birtwhistle, "Condition assessment of power transformer onload tap changers using wavelet analysis and self-organizing map: Field evaluation," *IEEE Trans. Power Del.*, vol. 18, no. 1, pp. 78–84, Jan. 2003.
[6] C. Gan, J. Wu, S. Yang, Y. Hu, and W. Cao, "Wavelet packet decomposition-based fault diagnosis scheme for SRM drives with a single current sensor," *IEEE Trans. Energy Convers.*, vol. 31, no. 1, pp. 303–313, Mar. 2016.
[7] X. Zhou and F. H. Wang, "Research on chaotic dynamic characteristics of onload tap changers," presented at the IEEE PES Gen. Meeting Conf. Exposit., National Harbor, MD, USA, Jul. 2014, pp. 1–5.
[8] P. Chen, X. Ma, F. Wang, F. Xie, and D. Zhou, "Mechanical fault diagnosis of on-load tap changer of power transformer by clustering algorithm," presented at the IEEE PES Asia–Pacific Power Energy Eng. Conf. (APPEEC), Kota Kinabalu, Malaysia, Oct. 2018, pp. 60–64.
[9] Z. Wu and N. E. Huang, "Ensemble empirical mode decomposition: A noise-assisted data analysis method," *Adv. Adapt. Data Anal.*, vol. 1, no. 1, pp. 1–41, 2008.
[10] Z. Long, N. Wu, H. Wang, and Q. Guo, "Turbo equalization based on a combined VMP-BP algorithm for nonlinear satellite channels," *IEEE Access*, vol. 6, pp. 35492–35500, 2018.
[11] F. Takens, "Detecting strange attractors in turbulence," in *Dynamical Systems and Turbulence*, vol. 898. New York, NY, USA: Springer-Verlag, 1981, pp. 366–381.
[12] S. Martin and C. T. M. Choi, "Nonlinear electrical impedance tomography reconstruction using artificial neural networks and particle swarm optimization," *IEEE Trans. Magn.*, vol. 52, no. 3, Mar. 2016, Art. no. 7203904.
[13] X. Niu, C. Yang, H. Wang, and Y. Wang, "Investigation of ANN and SVM based on limited samples for performance and emissions prediction of a CRDI-assisted marine diesel engine," *Appl. Thermal Eng.*, vol. 111, pp. 1353–1364, Jan. 2017.
[14] A. A. Bidgoli, H. E. Komleh, and S. J. Mousavirad, "Seminal quality prediction using optimized artificial neural network with genetic algorithm," presented at the 9th Int. Conf. Elect. Electron. Eng. (ELECO), Bursa, Turkey, Nov. 2015, pp. 695–699.
[15] *Guide to Operation and the Maintenance of Tap-Changers in the Transformer, DL/T 574-2010*, State Grid Corp. China, Beijing, China, 2010.
[16] F. B. Abid, S. Zgarni, and A. Braham, "Distinct bearing faults detection in induction motor by a hybrid optimized SWPT and aiNet-DAG SVM," *IEEE Trans. Energy Convers.*, vol. 33, no. 4, pp. 1692–1699, Dec. 2018.
[17] L. Cao, "Practical method for determining the minimum embedding dimension of a scalar time series," *Phys. D, Nonlinear Phenomena*, vol. 110, nos. 1–2, pp. 43–50, Dec. 1997.
[18] C.-W. Hsu and C.-J. Lin, "A comparison of methods for multiclass support vector machines," *IEEE Trans. Neural Netw.*, vol. 13, no. 2, pp. 415–425, Mar. 2002.
[19] A. M. Fraser and H. L. Swinney, "Independent coordinates for strange attractors from mutual information," *Phys. Rev. A, Gen. Phys.*, vol. 33, no. 2, pp. 1134–1140, Feb. 1986.
[20] M. Ohsaki, P. Wang, K. Matsuda, S. Katagiri, H. Watanabe, and A. Ralescu, "Confusion-matrix-based kernel logistic regression for imbalanced data classification," *IEEE Trans. Knowl. Data Eng.*, vol. 29, no. 9, pp. 1806–1819, Sep. 2017.
[21] C. Liu, P. Frazier, and L. Kumar, "Comparative assessment of the measures of thematic classification accuracy," *Remote Sens. Environ.*, vol. 107, no. 4, pp. 606–616, Apr. 2007.
[22] S. A. Bessedik, R. Djekidel, and A. Ameur, "Performance of different kernel functions for LS-SVM-GWO to estimate flashover voltage of polluted insulators," *IET Sci., Meas. Technol.*, vol. 12, no. 6, pp. 739–745, Sep. 2018.
[23] L. Wang, J. Liu, Y. Yan, X. Wang, and T. Wang, "Gas-liquid two-phase flow measurement using coriolis flowmeters incorporating artificial neural network, support vector machine, and genetic programming algorithms," *IEEE Trans. Instrum. Meas.*, vol. 66, no. 5, pp. 852–868, May 2016.

YUQIN XU was born in Kaifeng, Henan, China, in 1964. She received the bachelor's degree in electrical engineering and the Ph.D. degree from the Huazhong University of Science and Technology, Wuhan, in 1985 and 1988, respectively.

Since 1988, she has been with North China Electric Power University to study in electrical engineering. She is currently a Professor with the Electrical Engineering Department. She has studied in many areas of electrical engineering, such as power system relay protection and safety control, complex power system analysis, distributed generation, and microgrid.

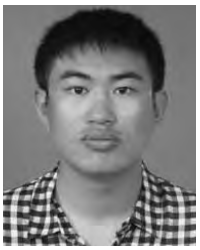

CONG ZHOU was born in Zhumadian, Henan, China, in 1995. He received the bachelor's degree in electrical engineering from North China Electric Power University, Baoding, in 2017, where he is currently pursuing the master's degree.

His tutor is Prof. Y. Xu. His current research interests include online detection and fault diagnosis of electrical equipment, and stability control of power systems.

JIANGHAI GENG, photograph and biography not available at the time of publication.

SHUGUO GAO, photograph and biography not available at the time of publication.

PING WANG, photograph and biography not available at the time of publication.